A Case Study for Imaging Complex Structures in the AndeanThrust Belt of Bolivia

Leandro Nicanoff and Yolanda Perez, RepsolYPF, Buenos Aires, Argentina, and Oz Yilmaz, Nanxun Dai, and Jie Zhang, GeoTomo LLC, Houston, Texas*

Summary

We designed an unconventionally unique seismic workflow entirely in shot-receiver domain to obtain an accurate earth model and earth image in areas with irregular topography, complex near-surface, and complex subsurface. We applied the workflow to 2-D seismic data from the Sub-Andean Thrust Belt of Bolivia and delineated a series of significant imbricate structures.

The data were acquired using a common-spread recording geometry whereby the receiver spread was fixed for most of the shots. A total of 1.260 receiver groups with 20,000-m maximum offset was placed along a nearly 33,000-m line traverse in the dominant structural dip direction at a 25-m interval. We included in the analysis a total of 518 shots at a 100-m interval along the line traverse, beginning at one end of the line. The topography is extremely rugged and elevations vary between 829-1,512 m along the line traverse.

The unique aspects of the analysis woırkflow are:

(1) The near-surface model is estimated by nonlinear tomography applied to first-arrival times that accounts for topography, and resolves lateral and vertical velocity variations. The corrections for the near-surface are performed by a combination of shot-receiver statics, *refraction-based* residual statics, and *wavefield datuming* --- an essential requirement for imaging from irregular topography.

(2) The subsurface modeling and prestack imaging are both performed from topography, not from a flat datum, based on rms and interval velocities estimated at *reflector* positions, not at *reflection* positions.

Introduction

The structures of the southern Sub-Andean Ranges of Bolivia owe their existence to the Andean Orogeny as a consequence of the regional compression produced by the subduction process that takes place at the plate boundary that lies along the Pacific Ocean margin of South America. The formation of nearly NS-trending Sub-Andean ranges began during the Miocene, while the frontal thrust is still deforming (McQuarrie et al., 2005). While some of the structures are characterized by tight folds, some are composed of multiple thrust sheets that diverge from each other. The structure of the southern Sub-Andean ranges is typically composed of two different structural levels divided by a major Devonian detachment zone. The most important aspect of the structural model is that the shallow structure may differ from the deep one. The objective in this case study is to delineate the imbricate structures associated with the Miocene overthrust tectonics.

Near-Surface Modeling

Starting with the field records, we picked the first-arrival times, checked the reciprocal errors and made sure that they are sufficiently small. Large reciprocal errors are often caused by geometry or picking errors. The reciprocal error for all shots varies between 5-25 ms with an average value of 12 ms. Next, we bundled the traveltime trajectories to form a general trend that is associated with laterally invariant but vertically varying velocities within the near surface. We picked a traveltime trajectory while honoring the change in gradient and determined the layer velocities and thicknesses for an initial model for the near-surface.

By performing a nonlinear traveltime tomography (Zhang and Toksoz, 1998) applied to picked first-arrival times, we estimated a final model for the near-surface. The *nonlinear* tomography solution is based on not just the first-arrival times, which may include wave types other than refraction, but also *changes* in traveltime gradient. In deriving a final model for the near-surface, the traveltime tomography is iterated until the difference between the modeled and the actual traveltimes, measured as the rms error in inversion, has been reduced to a sufficiently small value comparable to the reciprocal traveltime errors. We picked a floating datum and an intermediate datum that defines the interface between the near-surface and the subsurface. Also, we determined the replacement velocity taken as the lateral average of the velocities along the intermediate datum. For quality control to judge as to the acceptance of the near-surface model, we examined the raypaths associated with the final model and made sure that they do not hit the bottom of the model. Also, we examined the differences between the modeled traveltimes associated with the tomography solution for the near-surface and the observed (picked) traveltimes, and made sure that the discrepancy between the two traveltimes is minimal.

Signal Processing

We applied a parsimonious signal processing sequence to the shot records, and after each process, examined the average amplitude spectrum, time-variant spectrum, and the autocorrelogram for assessment and quality control of the processing parameters (Yilmaz, 2001). The signal processing includes t-squared scaling, predictive deconvolution, time-variant spectral whitening, trace balancing, and f-x dip filtering (Wang and West, 2001) of surface waves. Following the signal processing, by using the near-surface model, the floating datum and the intermediate datum, and the replacement velocity, we computed the shot and receiver statics. First, shots and receivers were moved down from topography to the intermediate datum using the velocity field associated with the near-surface; second, they were moved up to the floating datum using the replacement velocity. We then calculated and applied refraction-based shot and receiver residual statics (Zhang and Yilmaz, 2005). Shown in Figure 1 is a portion of a field record from the Bolivia line before and after the signal processing and near-surface corrections.

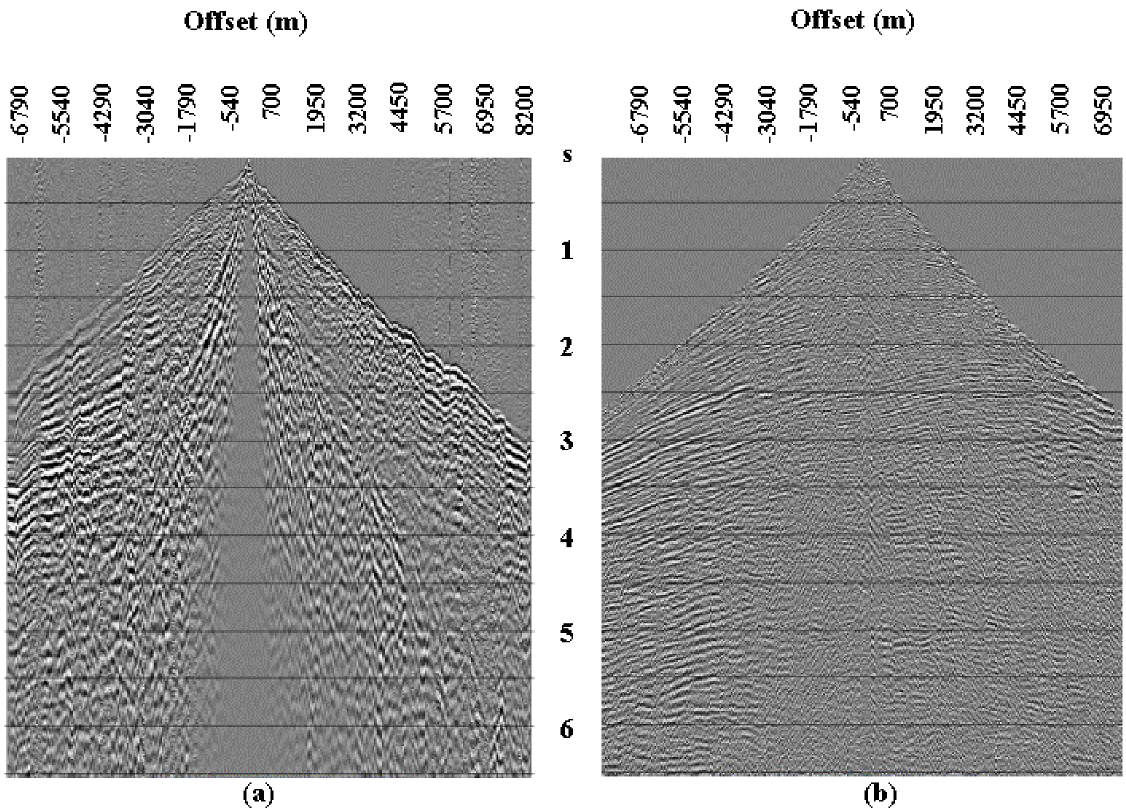

Figure 1. A portion of a field record from the Bolivia line: (a) Raw record with strong ground roll, (b) the same shot gather after signal processing that includes *t*-squared scaling, predictive deconvolution, time-variant spectral whitening, near-surface corrections and *f-x* dip filtering.

Subsurface Modeling and Imaging

We applied wavefield datuming to move the shots and receivers from the floating datum to a flat reference datum above the topography using the replacement velocity, and performed prestack time migration of shot gathers, equivalently from the floating datum, using a range of constant velocities. Next, we combined the constant-velocity migration panels to form an rms velocity volume (Shurtleff, 1984; Yilmaz, 2001; Yilmaz et al., 2005). We then interpreted this volume to derive an rms velocity field associated with events in their migrated positions. We display the three cross-sections of the velocity volume for picking the rms velocities (Figure 2). These are: the X-T plane --- distance along the line traverse versus event time after migration for a given rms velocity; the V-T plane --- rms velocity versus event time after migration for a specific location along the line traverse; and the V-X plane --- rms velocity versus distance along the line traverse for a specific time or horizon picked in the X-T window. While the X-T plane provides structural consistency, the V-X plane provides lateral consistency in picking the velocity strands. By combining the horizon strands picked in the X-T plane with the velocity strands picked from the horizon-consistent V-X windows, we created an rms velocity field associated with *reflector positions* (Figure 3). Finally, we performed prestack time migration of the shot gathers to verify the fidelity rms velocity field (Figure 4).

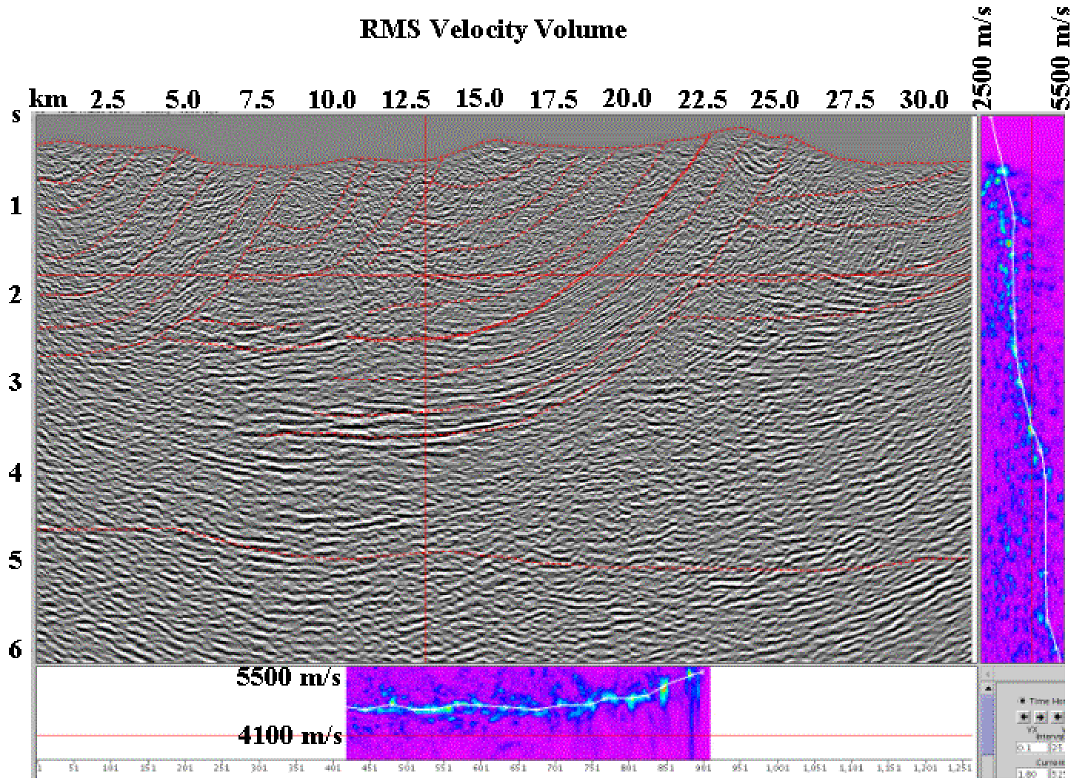

Figure 2. Three cross-sections of the rms velocity volume: X-T (center), V-T (right), and V-X (bottom). In this project, to create the rms velocity field, we combined the picks from the X-T planes for structural consistency and the V-X planes for lateral consistency.

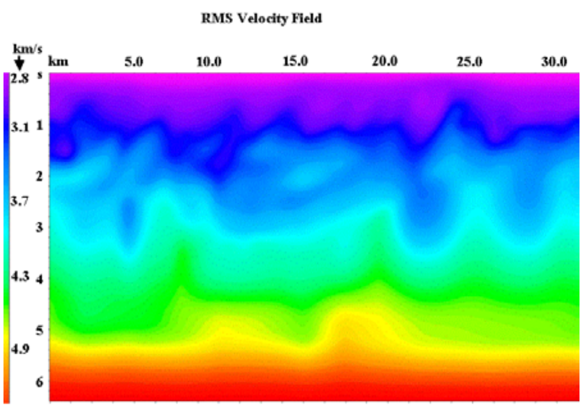

Figure 3. The rms velocity field derived from the picks from the X-T and V-X planes of the velocity volume shown in Figure 2.

Next, we unmigrated (demigrated) the resulting image from prestack time migration using the same rms velocity field as for prestack time migration. We performed Dix conversion of the rms velocities to derive an interval velocity field. We then performed poststack depth migration of the demigrated section using the interval velocity field and overlayed the image from poststack depth migration and the interval velocity field to check for consistency of the earth image with the earth model. Following the consistency check, we decided to use the interval velocity field based on Dix conversion to perform prestack depth migration of the shot gathers.

Conclusions

We picked the rms velocities from the velocity volume in a structurally consistent and laterally consistent manner (Figure 2). As such, note that the rms velocity field in Figure 3 indeed exhibits the structural features associated with overthrust tectonics in the area. Based on the observation that the image from prestack time migration is consistent with the rms velocity field, we also confirmed that the interval velocity field from Dix conversion also exhibits the structural behavior of overthurst tectonics. Specifically, the low-velocity zones coincident with the thrust fronts are attributed to weakening of rock strength as a result of the thrusting. Finally, the image from prestack depth migration turned out to be consistent with the image from prestack time migration, and both images enabled us to delienate the imbricate structures with high potential of hydrocarbons.

Acknowledgements

We are grateful to Repsol YPF for conducting this case study and granting the permission to publish the results.

References

McQuarrie, N., Horton, B. K., Zandt, G., Beck, S., and DeCelles, P. G., 2005, Lithospheric evolution of the Andean fold-thrust belt, Bolivai, and the origin of the central Andea Plateau, Tectonophysics, **399**, 15-37.

Shurtleff, R., 1984, An *F-K* procedure for prestack migration and velocity analysis: Presented at the 46th Ann. Mtg. European Asn. Expl. Geophys.

Wang, W. and West, G., 1991, F-X filters with dip rejection, Expanded Apbstracts, 61st Ann. Internat. Mtg., Soc. Expl. Geophys., 1436-1438.

Yilmaz, O., 2001, Seismic Data Analysis: Society of Exploration Geophysicists, Tulsa.

Yilmaz, O., Zhang, J., Pince, A., Aytunur, A., Elibuyuk, A., Uygun, S,, Onaran, T., Oner, A. F.,2005, A Large-Offset 2-D Seismic Survey for Imaging Imbricate Structures in Thrust Belts, Expanded Apbstracts, 75th Ann. Internat. Mtg., Soc. Expl. Geophys., 404-407.

Zhang, J. and Toksoz, M. N., 1998, Nonlinear refraction traveltime tomography: Geophysics, **63**, 1726-1737.

Zhang, J. and Yilmaz, O., 2005, Near-surface corrections for complex structure imaging, Expanded Apbstracts, 75th Ann. Internat. Mtg., Soc. Expl. Geophys., 2566-2568.

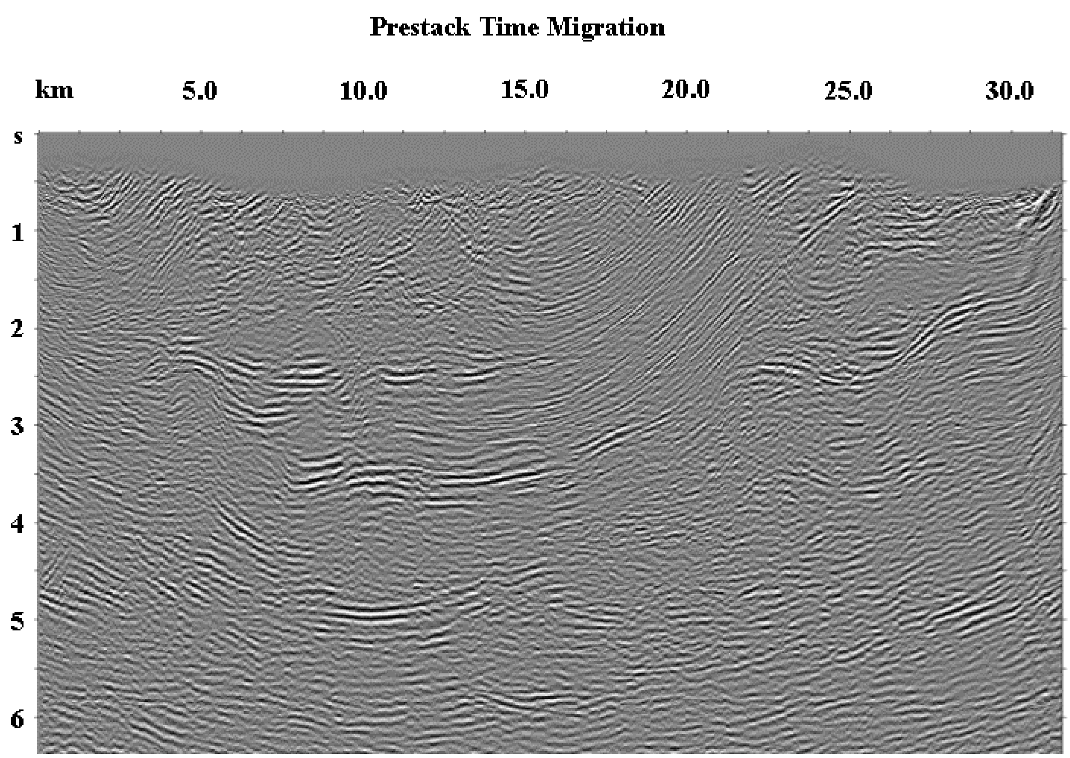

Figure 4. Prestack time migration using the rms velocity field shown in Figure 3.

EDITED REFERENCES

Note: This reference list is a copy-edited version of the reference list submitted by the author. Reference lists for the 2006 SEG Technical Program Expanded Abstracts have been copy edited so that references provided with the online metadata for each paper will achieve a high degree of linking to cited sources that appear on the Web.

REFERENCES

McQuarrie, N., B. K. Horton, G. Zandt, S. Beck, and P. G. DeCelles, 2005, Lithospheric evolution of the Andean fold-thrust belt, Bolivai, and the origin of the central Andea Plateau: Tectonophysics, **399**, 15–37.

Shurtleff, R., 1984, An F-K procedure for prestack migration and velocity analysis: 46th Annual Conference and Exhibition, EAGE, Extended Abstracts.

Wang, W., and G. West, 1991, F-X filters with dip rejection: 61st Annual International Meeting, SEG, Expanded Abstracts, 1436–1438.

Yilmaz, O., 2001, Seismic Data Analysis: SEG.

Yilmaz, O., J. Zhang, A. Pince, A. Aytunur, A Elibuyuk, S. Uygun, T. Onaran, and A. F. Oner, 2005, A large-offset 2-D seismic survey for imaging imbricate structures in thrust belts: 75th Annual International Meeting, SEG, Expanded Abstracts, 404–407.

Zhang, J., and M. N. Toksoz, 1998, Nonlinear refraction traveltime tomography: Geophysics, **63**, 1726–1737.

Zhang, J., and O. Yilmaz, 2005, Near-surface corrections for complex structure imaging: 75th Annual International Meeting, SEG, Expanded Abstracts, 2566–2568.